https://doi.org/10.1038/s41557-020-0423-6



Heteromeric three-stranded coiled coils designed using a Pb(II)(Cys)₃ template mediated strategy

Audrey E. Tolbert 16, Catherine S. Ervin 1,6, Leela Ruckthong 2,6, Thomas J. Paul 3,6, Vindi M. Javasinghe-Arachchige³, Kosh P. Neupane¹, Jeanne A. Stuckev⁴, Raieev Prabhakar⁶ and Vincent L. Pecoraro ^{1,5} □

Three-stranded coiled coils are peptide structures constructed from amphipathic heptad repeats. Here we show that it is possible to form pure heterotrimeric three-stranded coiled coils by combining three distinct characteristics: (1) a cysteine sulfur layer for metal coordination, (2) a thiophilic, trigonal pyramidal metalloid (Pb(II)) that binds to these sulfurs and (3) an adjacent layer of reduced steric bulk generating a cavity where water can hydrogen bond to the cysteine sulfur atoms. Cysteine substitution in an a site yields Pb(||)A₂B heterotrimers, while d sites provide pure Pb(||)C₂D or Pb(||)CD₂ scaffolds. Altering the metal from Pb(II) to Hg(II) or shifting the relative position of the sterically less demanding layer removes heterotrimer specificity. Because only two of the eight or ten hydrophobic layers are perturbed, catalytic sites can be introduced at other regions of the scaffold. A Zn(II)(histidine)₃(H₂O) centre can be incorporated at a remote location without perturbing the heterotrimer selectivity, suggesting a unique strategy to prepare dissymmetric catalytic sites within self-assembling denovo-designed proteins.

e novo protein design studies a wide range of protein systems in simplified peptidic environments¹⁻⁴. Bioinorganic constructs have been used to study the relationship between the protein scaffold and the function of a metal cofactor⁵⁻¹². A wide range of metal geometries and binding sites have been modelled in three-stranded coiled coils (3SCCs)¹³⁻²⁰. 3SCCs consist of amphipathic heptad repeats of amino acids (residues sequentially labelled **abcdefg**). Hydrophobic residues in the first (a) and fourth (d) positions form the core of the coiled coil, which is further stabilized by salt bridging between exterior residues in the fifth (e) and seventh (g) positions. Metal-binding sites result when any of the interior residues (a or d sites) are substituted with metal-binding residues. In the 3SCC these positions are designated **a** or **d** layers. Substitution of a Leu for a Cys generates a sulfur-rich heavy metal-binding site $^{13,18,20-22}$ while a His substitution generates a catalytic site like that of carbonic anhydrase (CA) or copper nitrite reductase (CuNiR)7,11,23,24

Our lab has previously reported the best aqueous peptidic models of both CA and CuNiR within these scaffolds10,23. The active site of CA consists of Zn(II) bound pseudo-tetrahedrally to three His ligands and an exogenous solvent molecule²⁵. The previously reported CA model performs to within 300-fold efficiency of the most active human enzyme, but does not reproduce critical acid/ base interactions due to the symmetry limitations imposed by the homotrimeric scaffold^{11,23,26-28}. Similarly, our CuNiR model accurately represents the first coordination sphere of the native enzyme, Cu bound to three His ligands and a water, but cannot model the second coordination sphere accurately^{24,29-32}. Attempts to include individual second coordination sphere residues are thwarted by the three-fold symmetry of the TRI scaffolds²⁴. Therefore, dissymmetric structures of the type A₂B or ABC are vital to the advancement of self-assembling de novo designed metalloproteins as many catalytic centres are dissymmetric in either the first or second coordination spheres, if not both. More generally, methods to prepare quantitatively and reliably dissymmetric scaffolds for different stoichiometries of self-assembling designed proteins are in their infancy.

Several groups have designed self-assembling, parallel, dissymmetric 3SCCs, but these constructs have either required substitution at each layer within the hydrophobic core or non-natural amino acids to ensure asymmetry³³⁻³⁵. Herein, we report a metal templating strategy using only coded amino acids that provides the first parallel, dissymmetric 3SCC modified within a single heptad. Although discussed specifically for 3SCCs, this approach underlines the general importance of metal template proteinprotein interactions (MTPPIs) as a mechanism to achieve dissymmetric assemblies^{36,37}. This new set of scaffolds provides a significant advance in metalloprotein design, allowing the preparation of dissymmetric metal-binding sites within the assembly, without costly non-natural residues. Our scaffolds require a cysteine layer for Pb(II) binding and a mixture of leucine and alanine residues in an adjacent layer (Table 1).

The interior of coiled-coil peptides contains hydrophobic residues in a desolvated core. Substitution of these residues for a metalbinding residue (for example, Cys, His, Asp) generates a 3SCC of reduced stability. Similarly, reducing the size of the side chain (for example, alanine) disrupts optimal packing and allows water to enter the core^{38,39}. Although building a metal-binding site in the centre of the coiled coil and allowing water into the hydrophobic core are both destabilizing, it is possible that when these modifications occur in tandem at adjacent layers, new stabilizing forces may result. Specifically, a symbiotic relationship between a hydrated alanine layer and metal-binding ligands can potentially lead to new hydrogen-bonding interactions that stabilize the system. We will show that this previously unappreciated cooperative interaction can

Department of Chemistry, University of Michigan, Ann Arbor, MI, USA. Department of Chemistry, Faculty of Science, King Mongkut's University of Technology, Thonburi (KMUTT), Bangkok, Thailand. ³Department of Chemistry, University of Miami, Coral Gables, FL, USA. ⁴Life Sciences Institute, University of Michigan, Ann Arbor, MI, USA. 5 Department of Biophysics, University of Michigan, Ann Arbor, MI, USA. 6 These authors contributed equally: Audrey E. Tolbert, Catherine S. Ervin. [™]e-mail: vlpec@umich.edu

Table 1 | List of abbreviations of representative peptide sequences with mutations shown in bold **Abbreviation** Peptide name **Full sequence** Ac-G WKALEEK LKALEEK LKALEEK G NH2 G Ac-G WKALEEK LKALEEK LKALEEK LKALEEK G-NH Ac-E WEALEKK LAALESK LOALEKK LEALEHG-NH2 Ac-E WEALEKK LAALESK LQALEKK LQALEKK LEALEHG-NH2 G-L12AL16CL30H G-A Ac-G WKALEEK LKAAEEK CKALEEK LKALEEK HKALEEK G-NH G-L16CL30H G-B Ac-G WKALEEK LKALEEK CKALEEK LKALEEK HKALEEK G-NH2 **G-**L12CL16A G-C Ac-G WKALEEK LKACEEK AKALEEK LKALEEK G-NH2 **G-**I 12C G-D Ac-G WKALEEK LKACEEK LKALEEK LKALEEK G-NH2 T-L12AL16C T-A Ac-G WKALEEK LKAAEEK CKALEEK LKALEEK G-NH2 **T-**L16C **T**-B Ac-G WKALEEK LKALEEK CKALEEK LKALEEK G-NH2 GC-L12AL16C GC-A Ac-E WEALEKK LAAAESK CQALEKK LQALEKK LEALEHG-NH2 GC-L16CL30H GC-B Ac-E WEALEKK LAALESK CQALEKK LQALEKK HEALEHG-NH2 GC-L12CL16A GC-C Ac-E WEALEKK LAACESK AQALEKK LQALEKK LEALEHGH2 **C**-L12C C-D Ac-E WEALEKK LAACESK LQALEKK LEALEHG-NH2 G-B_→ **G-**L16CL26TL30H Ac-G WKALEEK LKALEEK CKALEEK LKATEEK HKALEEK G-NH2 G-L16CL26DL30H G-B Ac-G WKALEEK LKALEEK CKALEEK LKADEEK HKALEEK G-NH

In the text, **a**-site peptides are designated A or B corresponding to whether they contain an alanine (A) or a leucine (B) above the cysteine, regardless of the remainder of the sequence. Similarly, **d**-site peptides are designated C or D corresponding to whether they contain an alanine (C) or a leucine (D) below the cysteine, regardless of the remainder of the sequence.

be exploited to generate A₂B type 3SCCs. The optimization of stability of this heterotrimeric scaffold will be shown to depend both on the hydrophobe, leucine, and the number of water molecules hydrogen-bonded to sulfur atoms within an internal cysteine laver that forms a trigonal pyramidal Pb(II)-S3 binding site. We will demonstrate that unique A₂B-type 3SCCs can be obtained with a templating Pb(II) ion either by utilizing a cysteine substitution in a d site, with an alanine placed at the subsequent a site (that is, C-XXX-A), or with an alanine in a d site preceding a cysteine substitution at an a site (that is, A-XXX-C). Reversing the order of the alanine/ cysteine modifications from these arrangements (that is, A-XX-C or C-XX-A) or substituting Hg(II) for Pb(II) no longer allows access to distinct A₂B type structures. Through crystallographic and computational analysis, we explain the mechanics behind this strategy for heterotrimer formation. We then demonstrate that the addition of a remote Zn(II)-His, site performs catalytic functions without perturbing heterotrimer formation.

Results and discussion

The objective of this study is to prepare parallel, heterotrimeric 3SCCs of the type A₂B by using a metal templating strategy that allows for further elaboration of the peptide assembly at locations remote from the templating metal region. With this aim, we have used three key components: Pb(II), which is known to form trigonal pyramidal structures within this class of 3SCCs³⁹⁻⁴¹; a layer of three cysteines incorporated either in an **a** type or **d** type layer to sequester the Pb(II); either Leu or Ala placed at a layer adjacent to cysteine-containing residues to effectuate hydrogen bonding between the cysteine sulfurs and water localized within the hydrophobic cavities of the scaffold. The driving force for attaining the desired A₂B constructs is the energetic competition between optimal packing of hydrophobes, such as Leu, and the stability obtained when water internalized within a hydrophobic cavity, formed with Ala, can hydrogen-bond to cysteine sulfur atoms coordinated to Pb(II).

X-ray crystal structures of the homotrimeric Pb(II) constructs provide insight into the formation of heterotrimeric constructs. Lead binds to both C-L12C (C-D) and GC-L16CL30H (GC-B) in *endo* conformations, meaning that both the Pb(II) and methane

carbons of cysteine are on the same side of the three-sulfur-atom plane (Table 1)39. In the d site (for example, G-D), the Pb(II) sits toward the N termini, above the cysteine plane, while in the a site (GC-B), the lead is displaced toward the C termini, below the cysteine plane. The introduction of an alanine layer adjacent to the cysteine layer, below a d site or above an a site, does not reorient the Pb(II) into a more spacious cavity; rather, three water molecules fill the void space allowing hydrogen bonding to each of the cysteine sulfurs (Fig. 1). In the a-site system, GC-L12AL16C (GC-A), water molecules are at hydrogen-bonding distances, ranging from 3.0 to 3.4 Å, but are still too far to interact directly with the Pb(II). This generates a water cavity that creates a stabilizing network of hydrogen bonds unique to the Ala-containing structure. Stability of the 3SCC is lost on removal of hydrophobic leucine packing in the absence of Pb(II) (Supplementary Fig. 1), but this hydrogen-bond network probably stabilizes the scaffold in the presence of Pb(II). When considering cysteines in **d** sites, **GC**-L12CL16A (**GC**-C) also has water present in the cavity left by introducing an alanine residue below the cysteine plane, but in a much different orientation (Fig. 1). Instead of the Cys-S bonding to two different water molecules aligned between each peptide strand, the space left from the Leu to Ala mutation allows for the association of a water 3.4 Å directly below each Cys residue (Fig. 1). Thus, in moving from an **a**-site Cys to a **d**-site Cys, a hydrogen-bonding network is still present but the network is constructed differently. The d-site system has fewer sulfur-water interactions and at different angles, explaining the difference in selectivity of the a- and d-site heterotrimers (vide infra). Once again, apo-G-C₃ is destabilized with respect to apo-G-D₃; however, Pb(II) binding to apo-G-C₃ provides both strong Pb(II)-S bonds to the aggregate and stabilizing hydrogen bonds, which should both strengthen the aggregate. Given these parent structures, we predicted that heterotrimeric structures could be obtained by balancing the stabilities achieved through knob-in-hole packing of leucines versus stabilizing the water hydrogen bonds to sulfur atoms coordinated to Pb(II) found in alanine-modified scaffolds.

To test this idea, the stabilities of the trimeric combinations of A–D type peptides were determined by quantum mechanics/ molecular mechanics (QM/MM) calculations. For both a- and

NATURE CHEMISTRY ARTICLES

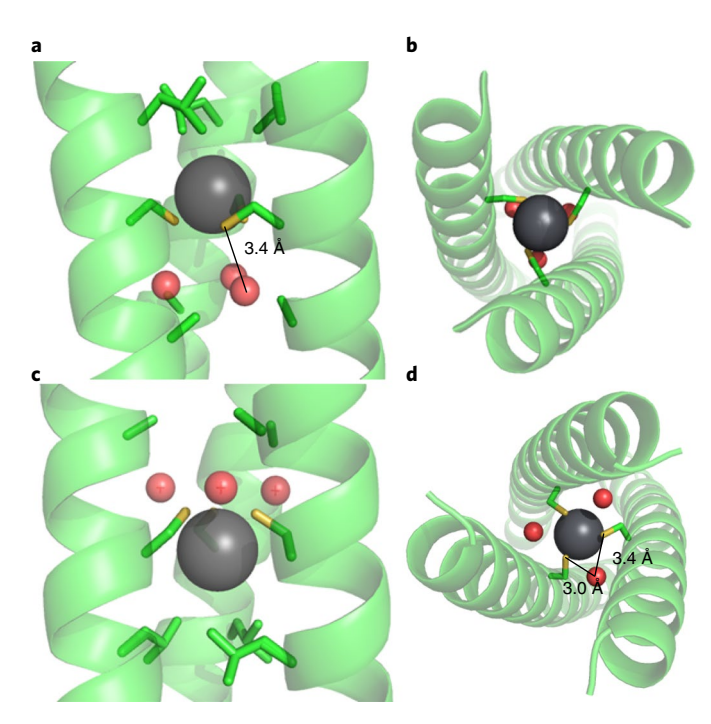


Fig. 1 | Ribbon diagrams of Pb(II)A3 (PDB: 6EGP) and Pb(II)C3 (PDB: 6MCD) 3SCCs with coordinated water residues. a,b, Pb(II) is shown as a large, dark grey sphere and water residues are shown as small, red spheres. Pb(II)C3 is shown from the side (a) and top (b) with the water-Cys distance of 3.4 Å shown as a solid line. **c,d**, Pb(II)A3 is shown from the side (c) and top (d) with water-Cys distances of 3.0 Å and 3.4 Å. The difference in the hydrogen-bonding networks of Pb(II)C3 and Pb(II)A3 are apparent in the position of the water and the number of hydrogen bonds to sulfur atoms formed by each. The region showing Zn(II) bound to the histidines has been omitted for clarity.

d-site constructs, the most stable scaffold is the 2 Ala:1 Leu heterotrimer (A₂B and C₂D forms). The structures represent the energy minima achieved through a combination of both hydrophobic packing and hydrogen bonding. In agreement with the different hydrogen-bonding networks observed by crystallography, there is a notable difference in the relative complexation energies of the a- and d -site constructs. In a-site constructs, where only one heterotrimer forms selectively, the energy differences between each trimer combination are much smaller than that for the **d**-site constructs (Table 2). The A₂B heterotrimer requires the least energy to complex, while the non-selective AB₂ heterotrimer complexes with 8.5 kcal mol⁻¹ more energy. The more favoured homotrimer, B₃, complexes with an additional 8.5 kcal mol-1 more energy than AB₂. The 3 Ala (A₃) homotrimer is the least energetically favourable with complexation energy 15 kcal mol-1 higher than the B₃ homotrimer. In the **d**-site constructs, however, the complexation energy differences are much greater between each scaffold. Again, the 2 Ala:1 Leu (C2D) 3SCC is the most favourable, while the 1 Ala:2 Leu (CD₂) complexes with 12.9 kcal mol⁻¹ more energy, which is slightly less favourable than AB2, the a-site 1 Ala:2 Leu complex. Importantly, the formation of the 3 Leu (D₃) trimer has been significantly destabilized in the **d** site, with a complexation energy $53.9\,kcal\,mol^{-1}$ higher than the most stable heterotrimer (C₂D) while the 3 Ala (C₃) trimer is 33 kcal mol⁻¹ higher, comparable to the A₃ trimer. As shown below, this negative design forces full selectivity in both heterotrimers as there is no competing structure with a small enough complexation energy to destabilize the desired assembly.

Table 2 | QM/MM calculations of complexation energies, 207 Pb NMR chemical shifts and Pb-S₃ p K_3 values of all constructs

Construct	Complexation energy (kcal mol ⁻¹) ^a	²⁰⁷ Pb NMR shift (ppm) ^b	pK _a ^c
A_3	32.0	5,574	10.88 ± 0.03
A_2B	0.0	5,597	10.55 ± 0.07
AB ₂	8.5	5,627, 5,595 (minor)	10.93 ± 0.11
B_3	17.0	5,645	11.65 ± 0.04
C ₃	33.0	5,762	11.23 ± 0.19
C_2D	0.0	5,875	11.6 ± 0.2
CD ₂	12.9	5,803	11.9 ± 0.2
D_3	53.9	5,789	11.7 ± 0.5

^aCalculated from GC peptides. ^bDetermined with G peptides. ^cDetermined with T peptides for A and B, and G peptides for C and D.

The energy differences between the **a**- and **d**-site complexes are due to the substantial structural differences in the Pb(II) forms of A₂B and C₂D heterotrimers. Again, both A₂B and C₂D bind lead in *endo* conformations, positioning the lead below the Cys plane in A₂B and above for C₂D. These coordination environments cause structural changes to the neighbouring mutation sites due to the differences in side-chain orientation and spacing between amino-acid layers (Fig. 2). For A₂B, the B-strand leucine reorients within the cavity to allow the Pb(II) coordination to remain fully symmetric. C₂D, however, maintains the orientation of the leucine but has a dissymmetric Pb(II) coordination. These differences in the coordination environments cause tighter packing and greater orbital overlap for the C₂D variant when compared with the neighbouring mutated residues for A₂B and C₂D.

The three water molecules present in the Pb(II) cavity also interact differently with the A and C peptides. In both A₃ and A₂B, the water molecules associate with the Cys-S and the backbone of Ala/Leu layer above and are oriented close to the helical interface. In C₃, however, the water molecules are oriented towards the interior of the helix and the hydrogen bond with each other and the Cys-S. In C₂D, the leucine residue disrupts this hydrogen bonding, resulting in the loss of a hydrogen bond to the D strand Cys-S. The stabilization of B₃ relative to A₃ is due to these water molecules interacting only with the side chains and backbones of the Cys residues and orienting closer to the helical interface. As a result, this structure contains more hydrogen bonds and provides more space to the bulky Leu residues than A3. The side chains of the Leu residues also minimize the steric clash by pointing down or to the exterior of B₃, making it more energetically favourable than A₃ (Supplementary Fig. 2). In contrast, the water molecules of both C₃ and D₃ are oriented more towards the interior of the helix and hydrogen-bond to each other and the Cys side chains. However, in D₃, these water molecules create a layer between Cys and Leu that sterically constrain the side chains of the Leu residues. Consequently, all 3 Leu residues are closely packed and their side chains are oriented towards the interior in this structure. This arrangement can destabilize the formation of D₃ over C₃ and further favours heterotrimer formation via negative design.

Given the reported X-ray structures of the relevant homotrimers and the subsequent computations for the relative energies of different mixed peptide species in the presence of Pb(II), we next considered whether one obtains exclusively the desired A₂B or C₂D heterotrimeric scaffolds experimentally. For the purposes of these studies, both **T** and **G** peptides were examined, giving comparable results, so only the **G** systems will be described in detail. First Pb(II) binding was tested for all homo- and heterotrimeric combinations

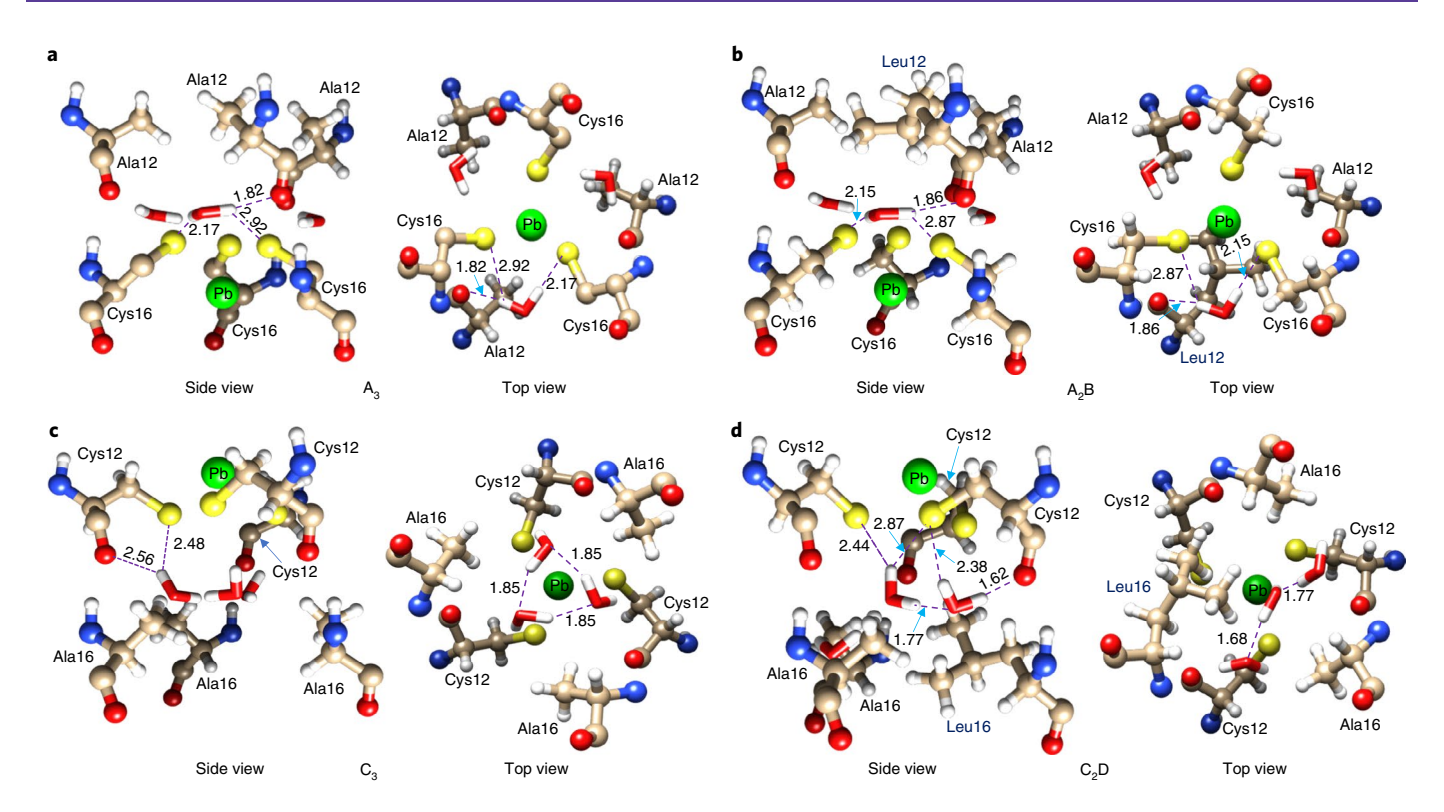


Fig. 2 | **Ball-and-stick models of the Cys and adjacent Ala/Leu layers for the 3 Ala and 2 Ala:1 Leu trimers. a-d**, The hydrogen-bonding interactions of A_3 (a), A_2 B (b), C_3 (c) and C_2 D (d) with the coordinated water molecules are shown in both side and top views. The Pb(11) remains fully symmetric in A_2 B, while the leucine of the D strand forces the Pb(11) to be asymmetric in C_2 D. This leucine also disrupts the hydrogen bonding to the D strand Cys-S.

using UV–vis spectroscopy. Spectra were obtained yielding the classic signatures for $Pb(II)S_3$ chromophores (Supplementary Fig. 3). Unfortunately, there are only small shifts in the UV band at $\sim\!340$ nm, so determination of the presence and ratios of different stoichiometric assemblies of peptides could not be determined. A more sensitive measure of species distribution can be obtained using ^{207}Pb NMR, which has a large chemical shift range, with Pb-S $_3$ signals spread over greater than 300 ppm (ref. 41). Using this highly sensitive technique, Pb(II) binding to binary mixtures of A and B peptides (or C and D) was investigated to assess whether pure A_2B or C_2D species could be formed.

Homotrimeric peptides containing **a**-site Cys (Pb(II)A₃ or Pb(II)B₃) are separated by ~75 ppm, with pure Pb(II)B₃ at 5,645 ppm and pure Pb(II)A₃ at 5,574 ppm (Fig. 3). The 2:1 mixtures of these peptides have chemical shifts evenly spaced within the range formed by these homotrimers. Pb(II)A₂B has a resonance at 5,597 ppm, 25 ppm downfield of Pb(II)A₃. Pb(II)AB₂ has two resonances. The major peak at 5,627 ppm is centred 25 ppm between the Pb(II)A₂B and Pb(II)B₃ assemblies. The minor resonance at 5,595 ppm corresponds to the Pb(II)A₂B peptide. Thus, formation of the Pb(II)A₂B is fully selective, while the 1 Ala:2 Leu heterotrimer is biased (we estimate ~80%) towards formation of the desired heterotrimer but lacks full selectivity. The low calculated energy gap between the desired and non-desired heterotrimer in this mixture explains the lack of selectivity. The non-desired Pb(II)A₂B complex is still able to form, but in small amounts due to the ratio of peptides in solution.

An alternative explanation for these observations is that the ^{207}Pb NMR is simply reporting a chemical shift for an average distribution of species that are coalescing to a single resonance. The two peaks seen for the Pb(II)AB2 conditions speak against this possibility; however, a more rigorous test is to perturb an existing signal by addition of one of the peptide components. Figure 3 shows how the spectra of a pure Pb(II)A2B system is altered by addition

of more A peptide to yield a stoichiometry of 5 A and 1 B peptide strands in the presence of two equivalents of lead. If coalescence were responsible for the observed intermediate signals, one would expect a single resonance shifted 12 ppm downfield of the Pb(II)A₂B peak, corresponding to a mixture that is 5/6 one homotrimer and 1/6 the other homotrimer. Instead, two peaks are observed that correspond to the resonances (5,597 ppm and 5,574 ppm) expected for Pb(II)A₂B and Pb(II)A₃ existing in a slow exchange equilibrium on the NMR timescale.

The d-site Cys-containing peptides also showed unique resonances for heterotrimeric mixtures of peptides, with all d-site resonances shifted significantly downfield (Supplementary Fig. 4). The homotrimeric peptides (in this case $Pb(II)C_3$ and $Pb(II)D_3$) are separated by only 30 ppm, with $Pb(II)C_3$ at 5,762 ppm and $Pb(II)D_3$ at 5,789 ppm. Interestingly, the resonances from heterotrimeric peptide mixtures fall downfield of the range of these two homotrimers. $Pb(II)CD_2$ is ~15 ppm downfield of $Pb(II)D_3$, at 5,803 ppm. Pb(II)C₂D is the most downfield-shifted at 5,875 ppm. As these resonances cannot have occurred from a mixture of homotrimeric signals, and because single peaks are observed in both cases, they must both correspond to fully selective heterotrimers. Heterotrimers therefore represent the peak stability from a mixture of hydrophobic packing of leucine residues and hydrogen bonding present from alanine residues when a **d**-site cysteine is employed. This is a consequence of the steep decrease in stability of the corresponding **d**-site homotrimers compared to the heterotrimeric scaffolds (Table 2). In the **a**-site constructs, full selectivity is only observed for Pb(II)A₂B, indicating that only this mixture has an energy minimum significant enough for complete formation of the desired heterotrimer.

UV spectra monitoring the pH titration of homo- and heterotrimeric systems provides further support for heterotrimer formation and illustrates the change in chemical properties associated with alanine substitution. The equilibrium examined is the release NATURE CHEMISTRY ARTICLES

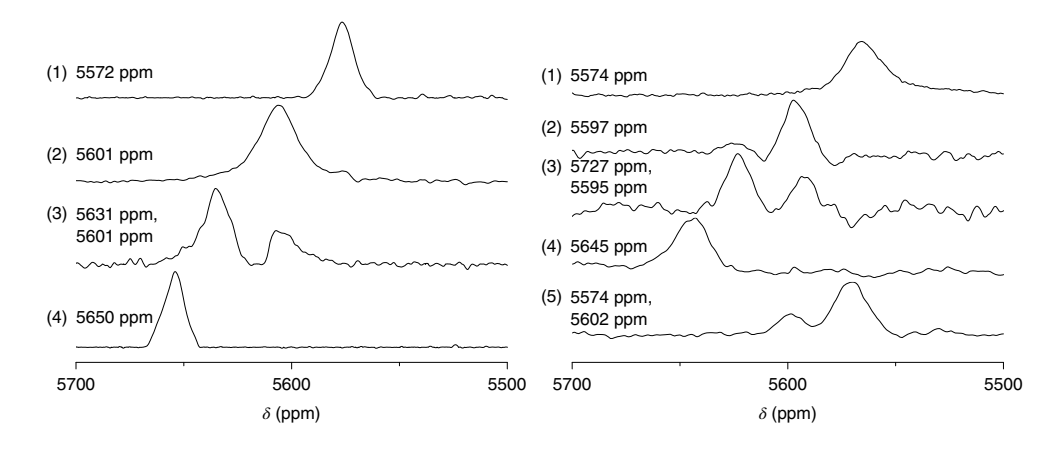


Fig. 3 | 207 Pb NMR of **T** and **G** peptides with a-site Cys residues. Left: 207 Pb NMR of **T** peptides A₃ (1), A₂B (2), AB₂ (3) and B₃ (4), showing the full selectivity of T-A₂B. Right: 207 Pb NMR spectra of **G** peptides A₃ (1), A₂B (2), AB₂ (3), B₃ (4) and A₅B (5) with 2 equiv. of 207 Pb(II), showing the full selectivity of **G**-A₂B as well as the coexistence of **G**-A₃ and **G**-A₂B to demonstrate the presence of asymmetric scaffolds rather than coalescence of symmetric signals.

of two protons, in a single step, to convert a Pb(II)S(SH)₂ peptide into the fully complexed Pb(II)S₃. Using T-L12AL16C (T-A) and T-L16C (T-B) for the series of Pb(II)A_nB_{3-n}, both heterotrimers have lower effective p K_a values than the calculated 2:1 mixtures of homotrimers (Fig. 4 and Table 2), demonstrating that a structure distinct from the homotrimers exists. The lower p K_a (10.55) for Pb(II)A₂B illustrates that this species most easily adapts the preferred Pb(II)S₃ structure. Interestingly, when Pb(II)C_nD_{3-n} peptides are titrated, the complexes containing leucine have p K_a values approximately equivalent to Pb(II)D₃, while Pb(II)C₃ has a slightly lower p K_a (Supplementary Fig. 5).

Mercury(II) has high affinity for thiolate ligation and will form trigonal planar structures in these 3SCCs^{18,39}. Nevertheless, selective formation of Hg(II)A₂B type heterotrimers cannot be achieved, as demonstrated by ¹⁹⁹Hg NMR of these systems (Supplementary Fig. 6). This is probably a consequence of the different numbers of waters in an alanine-generated cavity and the different hydrogen-bonding patterns these molecules form with the bound sulfur atoms. This also suggests that the apopeptides will not segregate in the absence of metal into these heterotrimeric assemblies, indicating that a trigonal pyramidal-type metal is essential. Additionally, positioning the alanine below an a-site cysteine does not lead to selectivity (Supplementary Fig. 7), indicating that proper water location relative to the lead is necessary for heterotrimer formation.

The addition of Zn(II) to the remote binding His, site of G-A and G-B (at the C-terminal end of the peptide) does not affect metal binding to the Cys, site, nor does it change the stoichiometry of the desired 3SCC (Supplementary Fig. 8)11. Therefore, this retention of $A_n B_{3-n}$ stoichiometry in the presence of a remote, catalytic metal ion allows for the study of catalysis in asymmetric coordination environments. The formation of heterotrimers was also found to be pH-independent, in the presence and absence of Zn(II), from 7.5 to 9.5, allowing for studies of p-nitrophenyl acetate (pNPA) hydrolysis at pH 9.5 (Supplementary Fig. 9). Lengthening the peptide from T to G resulted in a decrease in catalytic efficiency (~20%) of pNPA hydrolysis (Table 3) for the control G-B₃ homotrimer due to the increased stability of the helical bundle⁴², which decreased substrate access. The addition of a threonine residue to **G**-B in the d layer above the His residue was done to model T199 in native CAII. The homotrimer Pb(II)Zn(II)G-B_{T3} decreased the catalytic efficiency by a further 20%. We believe that this decreased activity is due to the methyl group of threonine rotating to the centre of the bundle and the hydroxy group pointing towards the helical interface (Supplementary Fig. 10). By including only a single T in a heterotrimeric Pb(II)Zn(II)G-A₂B_T, the rate increases to a value

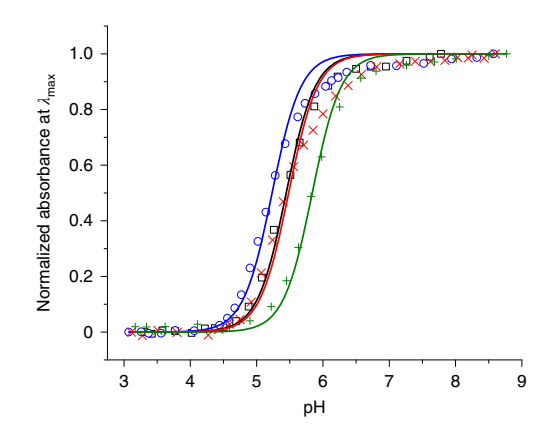


Fig. 4 | pH titration curves of Pb(\parallel)A $_n$ B $_{3-n}$ scaffolds at λ_{max} for homoand heterotrimers. Symbols are data points and solid lines are fits to the equation in the Supplementary Information showing the acid-shifted pK $_a$ values for heterotrimers based on the calculated ratios of homotrimeric signals. Pb(\parallel)A $_3$ is represented by open squares, Pb(\parallel)A $_2$ B by open circles, Pb(\parallel)AB $_2$ with \times symbols and Pb(\parallel)B $_3$ with + symbols. pK $_a$ values, calculated for each fit assuming an equilibrium Pb(\parallel)(H $_2$ A $_n$ B $_{n-3}$) \rightarrow Pb(\parallel) A $_n$ B $_{n-3}$ + 2H $^+$, are provided in Table 2.

exceeding the Pb(II)Zn(II)G-B_{T3} by $\sim 30\%$ and is superior to the parent Pb(II)Zn(II)G-B₃ homotrimer. This increase shows the modest, but significant effect that asymmetry can have on catalysis. To combat the complication of side-chain orientation with T residues, we instead examined the effect of aspartate coordination on catalysis. We reasoned that the aspartate side chain was too short to directly bind to the Zn(II) when three histidines were coordinated to the metal, but would provide an oxygen that could serve as an acid-base catalyst, similar to T199. With three additional Asp residues Pb(II) Zn(II)**G**- B_{D3} , a 25% increase in catalytic efficiency is seen over Pb(II) Zn(II)G-B₃. Although a slight, though statistically insignificant, increase is seen with just a single Asp residue Pb(II)Zn(II)G-A2BD as compared to $Pb(II)Zn(II)G-B_{D3}$, both of these peptides match or exceed the catalytic efficiency of the original Pb(II)Zn(II)T-B₃ and are over 40% better than $Pb(II)Zn(II)G-B_{T3}$. Although only modest changes in catalytic efficiency are illustrated with these examples, one can imagine larger effects with more drastic modifications that could be achieved in future designs.

We have presented a novel approach to achieve selectivity for supramolecular assembly in designed proteins by combining three

Table 3 | Kinetic values for pNPA ester hydrolysis at pH 9.5 for Pb(\shortparallel) and Zn(\shortparallel) bound peptides

Peptide	$k_{\rm cat}/K_{\rm M}$ (M ⁻¹ s ⁻¹)	$k_{\rm cat}$ (s ⁻¹)	$K_{\rm M}$ (mM)	
T-B ₃ ^a	23.3 ± 0.3	0.040 ± 0.012	1.7 ± 0.5	
G -B ₃	18.5 ± 0.6	0.064 ± 0.007	3.5 ± 0.5	
G -B _{T3}	14.8 ± 1.4	0.056 ± 0.026	3.8 ± 2.1	
\mathbf{G} - $\mathbf{A}_2\mathbf{B}_{T}$	20.6 ± 2.1	0.030 ± 0.007	1.5 ± 0.7	
G -B _{D3}	24.2 ± 2.5	0.024 ± 0.004	1.0 ± 2.0	
$G-A_2B_D$	25.1 ± 2.5	0.021 ± 0.003	0.8 ± 0.2	
²Full-seauence T L9CL23H [™] .				

distinct features: (1) a cysteine sulfur layer for metal coordination, (2) a thiophilic, trigonal pyramidal metalloid (Pb(II)) that binds to these sulfurs and (3) an adjacent layer of reduced steric bulk within the hydrophobic core allowing a cavity that contains waters that hydrogen-bond to the cysteine sulfur atoms. When combined properly, peptides with a-site cysteine substitution yield A₂B heterotrimers exclusively, and when cysteine is in the **d** site, either pure C₂D or CD₂ scaffolds are obtained. Altering the metal from Pb(II) to Hg(II) or shifting the relative position of the sterically less demanding side chain removes heterotrimer selectivity. These studies illustrate the importance of solvent-based molecules for stabilizing protein-protein interactions that define the appropriate scaffold assembly. Finally, incorporating a bulky side chain, such as histidine, at a remote location within the coiled coil, and even binding a metal such as Zn(II) at that site, does not perturb the ability to obtain the desired heterotrimers. Thus, these studies provide a unique strategy to prepare dissymmetric catalytic sites within self-assembling de novo designed proteins. Further studies will explore the behaviour of metals in these remote sites and examine whether this strategy can be extended to other coiled coils of different stoichiometries.

Online content

Any Nature Research reporting summaries, source data, extended data, supplementary information, acknowledgements, peer review information; details of author contributions and competing interests; and statements of data and code availability are available at https://doi.org/10.1038/s41557-020-0423-6.

Received: 9 January 2019; Accepted: 19 January 2020; Published online: 02 March 2020

References

- Bryson, J. W. et al. Protein design: a hierarchic approach. Science 270, 935–941 (1995).
- Bryson, J. W., Desjarlais, J. R., Handel, T. M. & Degrado, W. F. From coiled coils to small globular proteins: design of a native-like three-helix bundle. *Protein Sci.* 7, 1404–1414 (1998).
- Tripet, B., Wagschal, K., Lavigne, P., Mant, C. T. & Hodges, R. S. Effects of side-chain characteristics on stability and oligomerization state of a de novo-designed model coiled-coil: 20 amino acid substitutions in position 'd'. J. Mol. Biol. 300, 377–402 (2000).
- Walsh, S. T. R., Cheng, H., Bryson, J. W., Roder, H. & DeGrado, W. F. Solution structure and dynamics of a de novo designed three-helix bundle protein. *Proc. Natl Acad. Sci. USA* 96, 5486–5491 (1999).
- Kaplan, J. & DeGrado, W. F. De novo design of catalytic proteins. Proc. Natl Acad. Sci. USA 101, 11566–11570 (2004).
- Reig, A. J. et al. Alteration of the oxygen-dependent reactivity of de novo Due Ferri proteins. Nat. Chem. 4, 900–906 (2012).
- Tegoni, M., Yu, F., Bersellini, M., Penner-Hahn, J. E. & Pecoraro, V. L. Designing a functional type 2 copper center that has nitrite reductase activity within α-helical coiled coils. *Proc. Natl Acad. Sci. USA* 109, 1–6 (2012).
- Faiella, M. et al. An artificial di-iron oxo-protein with phenol oxidase activity. Nat. Chem. Biol. 5, 882–884 (2009).

- Lombardi, A. et al. Retrostructural analysis of metalloproteins: application to the design of a minimal model for diiron proteins. *Proc. Natl Acad. Sci. USA* 97, 6298–6305 (2000).
- Zastrow, M. L. & Pecoraro, V. L. Designing functional metalloproteins: from structural to catalytic metal sites. *Coord. Chem. Rev.* 257, 2565–2588 (2013).
- Zastrow, M. L., Peacock, A. F., Stuckey, J. A. & Pecoraro, V. L. Hydrolytic catalysis and structural stabilization in a designed metalloprotein. *Nat. Chem.* 4, 118–123 (2011).
- Yu, F. et al. Protein design: toward functional metalloenzymes. Chem. Rev. 114, 3495–3578 (2014).
- 13. Dieckmann, G. R. et al. De novo design of mercury-binding two- and three-helical bundles. *J. Am. Chem. Soc.* **119**, 6195–6196 (1997).
- Dieckmann, G. R. et al. The role of protonation and metal chelation preferences in defining the properties of mercury-binding coiled coils. J. Mol. Biol. 280, 897–912 (1998).
- Murase, S., Ishino, S., Ishino, Y. & Tanaka, T. Control of enzyme reaction by a designed metal-ion-dependent α-helical coiled-coil protein. *J. Biol. Inorg. Chem.* 17, 791–799 (2012).
- Kiyokawa, T. et al. Binding of Cu(II) or Zn(II) in a de novo designed triple-stranded α-helical coiled-coil toward a prototype for a metalloenzyme. *J. Pept. Res.* 63, 347–353 (2004).
- Farrer, B. T. & Pecoraro, V. L. Hg(II) binding to a weakly associated coiled coil nucleates an encoded metalloprotein fold: a kinetic analysis. *Proc. Natl Acad. Sci. USA* 100, 3760–3765 (2003).
- Matzapetakis, M. et al. Comparison of the binding of cadmium(II), mercury(II) and arsenic(III) to the de novo designed peptides TRI L12C and TRI L16C. J. Am. Chem. Soc. 124, 8042–8054 (2002).
- Matzapetakis, M. De Novo Design of Heavy Metal Binding Proteins (Univ. Michigan, 2004).
- Matzapetakis, M., Ghosh, D., Weng, T.-C., Penner-Hahn, J. E. & Pecoraro, V. L. Peptidic models for the binding of Pb(II), Bi(III) and Cd(II) to mononuclear thiolate binding sites. J. Biol. Inorg. Chem. 11, 876–890 (2006).
- Farrer, B. T., McClure, C. P., Penner-Hahn, J. E. & Pecoraro, V. L. Arsenic(III)-cysteine interactions stabilize three-helix bundles in aqueous solution. *Inorg. Chem.* 39, 5422–5423 (2000).
- Iranzo, O., Cabello, C. & Pecoraro, V. L. Heterochromia in designed metallopeptides: geometry-selective binding of Cd(II) in a de novo peptide. Angew. Chem. Int. Ed. 46, 6688–6691 (2007).
- Zastrow, M. L. & Pecoraro, V. L. Influence of active site location on catalytic activity in de novo-designed zinc metalloenzymes. *J. Am. Chem. Soc.* 135, 5895–5903 (2013).
- Koebke, K. J. et al. Modifying the steric properties in the second coordination sphere of designed peptides leads to enhancement of nitrite reductase activity. *Angew. Chem. Int. Ed.* 57, 3954–3957 (2018).
- Maren, T. H. Carbonic anhydrase: chemistry, physiology, and inhibition. Physiol. Rev. 47, 597–781 (1967).
- Kiefer, L. L., Paterno, S. A. & Fierke, C. A. Hydrogen bond network in the metal binding site of carbonic anhydrase enhances zinc affinity and catalytic efficiency. J. Am. Chem. Soc. 117, 6831–6837 (1995).
- Liang, Z., Xue, Y., Behravan, G., Jonsson, B.-H. & Lindskog, S. Importance
 of the conserved active-site residues Try7, Glu106 and Thr199 for the
 catalytic function of human carbonic anhydrase II. *Eur. J. Biochem.* 211,
 821–827 (1993).
- Xue, Y., Liljas, A., Jonsson, B. & Lindskog, S. Structural analysis of the zinc hydroxide-Thr-199-Glu-106 hydrogen-bond network in human carbonic anhydrase II. *Proteins* 17, 93–106 (1993).
- Kukimoto, M. et al. X-ray structure and site-directed mutagenesis of a nitrite reductase from *Alcaligenes faecalis* S-6: roles of two copper atoms in nitrite reduction. *Biochemistry* 33, 5246–5252 (1994).
- Murphy, M. E. P., Turley, S. & Adman, E. T. Structure of nitrite bound to copper-containing nitrite reductase from *Alcaligenes faecalis*: mechanistic implications. *J. Biol. Chem.* 272, 28455–28460 (1997).
- Li, Y., Hodak, M. & Bernholc, J. Enzymatic mechanism of copper-containing nitrite reductase. *Biochemistry* 54, 1233–1242 (2015).
- Libby, E. & Averill, B. A. Evidence that the Type 2 copper centers are the site of nitrite reduction by *Achromobacter cycloclastes* nitrite reductase. *Biochem. Biophys. Res. Commun.* 187, 1529–1535 (1992).
- 33. Kiyokawa, T. et al. Selective formation of AAB- and ABC-type heterotrimeric α -helical coiled coils. *Chemistry* **10**, 3548–3554 (2004).
- Schnarr, N. A. & Kennan, A. J. Peptide Tic-Tac-Toe: heterotrimeric coiled-coil specificity from steric matching of multiple hydrophobic side chains. J. Am. Chem. Soc. 124, 9779–9783 (2001).
- Schnarr, N. A. & Kennan, A. J. Coiled-coil formation governed by unnatural hydrophobic core side chains. J. Am. Chem. Soc. 123, 11081–11082 (2001).
- Bailey, J. B., Subramanian, R. H., Churchfield, L. A. & Tezcan, F. A. Metal-directed design of supramolecular protein assemblies. Methods Enzymol. 580, 223–250 (2016).

NATURE CHEMISTRY ARTICLES

- Song, W. J., Yu, J. & Tezcan, F. A. Importance of scaffold flexibility/rigidity in the design and directed evolution of artificial metallo-beta-lactamases. J. Am. Chem. Soc. 139, 16772–16779 (2017).
- Harbury, P. B., Zhang, T., Kim, P. S. & Alber, T. A switch between twothree-, and four-stranded coiled coils in GCN4 leucine zipper mutants. *Science* 262, 1401–1407 (1993).
- Ruckthong, L., Zastrow, M. L., Stuckey, J. A. & Pecoraro, V. L. A crystallographic examination of predisposition versus preorganization in de novo designed metalloproteins. J. Am. Chem. Soc. 138, 11979–11988 (2016).
- Neupane, K. P. & Pecoraro, V. L. Pb-207 NMR spectroscopy reveals that Pb(II) coordinates with glutathione (GSH) and tris cysteine zinc finger proteins in a PbS₃ coordination environment. *J. Inorg. Biochem.* 105, 1030–1034 (2011).
- Neupane, K. P. & Pecoraro, V. L. Probing a homoleptic PbS₃ coordination environment in a designed peptide using ²⁰⁷Pb NMR spectroscopy: implications for understanding the molecular basis of lead toxicity. *Angew. Chem. Int. Ed.* 49, 8177–8180 (2010).
- Ruckthong, L., Deb, A., Hemmingsen, L., Penner-Hahn, J. E. & Pecoraro, V. L. Incorporation of second coordination sphere d-amino acids alters Cd(II) geometries in designed thiolate-rich proteins. *J. Biol. Inorg. Chem.* 23, 123–135 (2018).

Publisher's note Springer Nature remains neutral with regard to jurisdictional claims in published maps and institutional affiliations.

© The Author(s), under exclusive licence to Springer Nature Limited 2020

Data availability

Protein crystallographic datasets are available from the Protein Data Bank under accession codes 6EGP and 6MCD. The authors declare that all other data supporting the findings of this study are available within the Article and its Supplementary Information.

Acknowledgements

We thank J. Meager for her help with crystal data collection. We also thank The CCP4/ APS School in Macromolecular Crystallography, from data collection to structure refinement and beyond 2016 for their help with crystal data processing. We acknowledge funding from NIH grant no. R01 ES012236, NSF grant no. CHE-1664926 and the Skill Development Grant from King Mongkut's University of Technology, Thonburi, Thailand. Use of the Advanced Photon Source, an Office of Science User Facility operated for the US Department of Energy (DOE) Office of Science by Argonne National Laboratory, was supported by the US DOE under contract no. DE-AC02-06CH11357. Use of LS-CAT Sector 21 was supported by the Michigan Economic Development Corporation and the Michigan Technology Tri-Corridor (grant no. 085P1000817).

Author contributions

A.E.T. and C.S.E. performed experiments and contributed equally to manuscript preparation. L.R. and J.A.S. performed crystallography work and L.R. contributed to manuscript preparation. T.J.P., V.M.J.-A. and R.P. performed QM/MM calculations and R.P. contributed to manuscript preparation. L.R. and T.J.P. contributed equally to this manuscript. K.P.N. performed experiments. V.L.P. directed research and contributed to manuscript preparation.

Competing interests

The authors declare no competing interests.

Additional information

Supplementary information is available for this paper at https://doi.org/10.1038/s41557-020-0423-6.

Correspondence and requests for materials should be addressed to V.L.P.
Reprints and permissions information is available at www.nature.com/reprints.